Stability Investigation of Se- and Te-Substituted Tetrahedrite

Hailong Yang, Marie-Christine Record, Ziya Aliev, Pascal Boulet

▶ **To cite this version:**

Hailong Yang, Marie-Christine Record, Ziya Aliev, Pascal Boulet. Stability Investigation of Se- and Te-Substituted Tetrahedrite. Journal of Electronic Materials, 2020, 49 (6), pp.3566-3576. 10.1007/s11664-020-08043-8 . hal-02507691

HAL Id: hal-02507691
https://hal.science/hal-02507691

Submitted on 10 Feb 2022

HAL is a multi-disciplinary open access archive for the deposit and dissemination of scientific research documents, whether they are published or not. The documents may come from teaching and research institutions in France or abroad, or from public or private research centers.

L'archive ouverte pluridisciplinaire **HAL**, est destinée au dépôt et à la diffusion de documents scientifiques de niveau recherche, publiés ou non, émanant des établissements d'enseignement et de recherche français ou étrangers, des laboratoires publics ou privés.

Stability investigation of Se- and Te-substituted tetrahedrite

Hailong Yang [1,2], Marie-Christine Record[2,*], Ziya Aliev[3], Pascal Boulet[1]

[1] Aix-Marseille Univ., CNRS, MADIREL, Marseille, France

[2]Aix-Marseille Univ., CNRS, IM2NP, Marseille, France

[3]Azerbaijan State Oil and Industry University, AZ1010 Baku, Azerbaijan

* corresponding author : m-c.record@univ-amu.fr

DFT (density functional theory) and QTAIM (quantum theory of atoms in molecules) calculations have been performed to investigate the influence of Se and Te substitutions on the stability of tetrahedrite. The formation energies, the laplacian of the electron density, the total and local volume changes and the site charges ones have been determined. The DFT results show that the single atom substitution is the most preferred one and that selenium is preferred for sulphur replacement whereas antimony can be equally replaced by selenium and tellurium. However as selenium substitutes for either sulphur or antimony, QTAIM calculations evidenced large structural and chemical changes in the strutures. Additional experimental results, in agreement with QTAIM ones, allow us to conclude that the investigation of alloys stability can not be limited to DFT calculations of formation energies and total volume changes. QTAIM appears as a valuable complementary method to get information on phase stabilities.

Key words: Cu-Sb-S system; substituted tetrahedrite; phase stability; DFT; QTAIM

INTRODUCTION

Copper antimony chalcogenides have high potentialities as semiconductors for electro-optic devices, thermoelectric devices, optical recording media and sustainable solar cell. As examples we can mention Cu_3SbSe_3 which has enormously drawn attention of the researchers in the thermoelectric field because of its ultra-low lattice thermal conductivity, and the Cu-Sb-S compounds that are modern state-of-the-art thermoelectric materials for midtemperature heat-to-power conversion with the advantage of being environmental friendly. The thermoelectric figure of merit zT for many doped and natural tetrahedrite materials ($Cu_{12}Sb_4S_{13}$) gets close to unity at 450°C ; this value is comparable to that of conventional p-type TE materials. However because of the complexity of the Cu-Sb-S phase diagram around the $Cu_{12}Sb_4S_{13}$ composition, these materials are always constituted of several phases for which the proportions generally differ from a sample to another one. The large scale use of tetrahedrite for thermoelectric applications necessitates the mastering of the properties and thus the mastering of the material constitution. A way could be to extend the composition range of the tetrahedrite stability. To reach this goal, we investigated the stability of various substituted tetrahedrites in which S atoms were replaced by Se and/or Te ones. This work was mainly carried out by coupled DFT and QTAIM calculations and complemented by some experiments.

THE Cu-Sb-S SYSTEM

Information on the constitutive binary systems Sb-S, Cu-S and Cu-Sb can be found in Ref. 1-6, Ref. 7-8 and Ref. 9-11, respectively. The Sb-S phase diagram only shows one condensed stable binary phase Sb_2S_3 (stibnite) with a congruent melting and two regions of liquid immiscibility. The Cu-S binary system contains three intermediate phases, namely Cu_2S (chalcocite), Cu_9S_5 (digenite) and CuS (covellite) and a solid solution between digenite

and chalcocite extending from 83 to 1129°C. Numerous phases have also been identified at low temperatures (<103°C) but considerable uncertainties still remain both on the stability range of the digenite and on the temperatures of phase transitions in the low temperature range. Moreover no studies on the stability of the new minerals as roxbyite ($Cu_{1.78}S$), geerite ($Cu_{1.6}S$) and spionkopite ($Cu_{1.4}S$) have been performed. There are several intermediate phases in the Cu-rich region but only two (δ and η) exist at room temperature.

Phase stability and phase relations in the Cu-Sb-S ternary system have been studied by numerous authors.[3,12-19] There are four compounds in the Cu-Sb-S ternary system, namely $CuSbS_2$ (chalcostibite), Cu_3SbS_3 (skinnerite), Cu_3SbS_4 (famatinite), and $Cu_{12}Sb_4S_{13}$ (tetrahedrite). Chalcostibite, $CuSbS_2$, forms readily by reaction from the elements and did not show any composition range.[3] By contrast, Golovei *et al.*[20] found a homogeneity range for $CuSbS_2$ and a polymorphic transformation. Skinnerite was first reported by Godolikov *et al.*[17] who prepared it by sintering Cu_2S and Sb_2S_3 at 480°C and 530°C. It has the ideal composition of Cu_3SbS_3 with a small composition field along the line Cu_2S-Sb_2S_3 at 500°C. Karup-Møller *et al.*[21] have found these ore aggregates crystallized at about 400°C from metal-rich residual magmatic fluids markedly deficient in sulfur. Cu_3SbS_3 is stable in the Cu-Sb-S system in the temperature range 359-607°C. Below 359°C this phase decomposes into a mixture of native antimony, chalcostibite and tetrahedrite,[3] but if it is cooled slowly, it decomposes to give a mixture of tetrahedrite, antimony and digenite.[22] At 607°C, Cu_3SbS_3 congruently melts. Pfitzner[23] have investigated both the high and low-temperature phases. The high-temperature modification is disordered and stable above 122°C, and is supposed to show high copper ion conductivity or at least a high copper diffusion coefficient. The low-temperature form is ordered and stable below -9°C. Famatinite, Cu_3SbS_4, derived from sphalerite, melts congruently at 627°C, and is not known to have any stable polymorph forms.[3] The only compound with an extensive composition field in the Cu-Sb-S system is tetrahedrite. The

basic structure of minerals of the tetrahedrite group was solved by Pauling and Newman[24] and now the widely accepted formula $Cu_{12}Sb_4S_{13}$ represented its composition. As for the Pauling and Neuman formula, $Cu_{12+x}Sb_{4+y}S_{13}$, where $0 \leq x \leq 1.92$ and $-0.02 \leq y \leq 0.27$, there is no clear evidence so far proving the substitution schemes implied in this formula are correct.[24] Cambi and Elli[14] have given an extreme composition range for tetrahedrites going from $4Cu_2S \cdot Sb_2S_3$ to $3Cu_2S \cdot Sb_2S_3$ (i.e. $Cu_8Sb_2S_7$ to Cu_3SbS_3). Since Skinner *et al.*[3] have not managed to prepare a single homogenous phase with the composition $Cu_{12}Sb_4S_{13}$, they believed that this phase has a stability temperature range below 300°C. These authors also found that the unit cell edges of tetrahedrite decrease with the sulfur content. Tatsuka and Morimoto[25] reported the formation of pseudo-tetrahedrite (T'_3) which is stable between 250 and 350°C and is a superlattice of $Cu_{12+x}Sb_{4+y}S_{13}$ (T_3) (lattice parameter of T'_3 is twice that of T_3). Along the Cu_2S-Sb_2S_3 section reported by Chang *et al.*,[26] the composition of pseudo-tetrahedrite ranges from Cu_3SbS_3 to $Cu_{12.39}Sb_{4.54}S_{13}$. Below 250°C, a prolonged annealing of T_3 or T'_3 results in a phase mixture consisting of Cu_3SbS_4, $Cu_{2-x}S$ and Sb. Makowicky and Skinner[27] have confirmed that tetrahedrite has two room-temperature phases Cu-poor phase $Cu_{12.3}Sb_4S_{13}$ and Cu-rich phase $Cu_{13.8}Sb_4S_{13}$ produced by a low-temperature exsolution of tetrahedrite $Cu_{12.59}Sb_{4.03}S_{13}$. However when melts, whose compositions lie near that of tetrahedrite, are cooled at the rate of 50-100°C/h, instead of separation of the phase Cu_3SbS_3, metastable solid tetrahedrite solutions crystallize out and then decompose to phases with a complex structure, which are absent in the phase diagram.[28] The crystal structure of stoichiometric tetrahedrite $Cu_{12}Sb_4S_{13}$ was determined for the first time by Skinner *et al.*[3] There is no phase transitions for $Cu_{12}Sb_4S_{13}$ up to 300°C, and the two exsolution phases $Cu_{12.3}Sb_4S_{13}$ and $Cu_{13.8}Sb_4S_{13}$ show a high copper-ion mobility even at room temperature. According to [29] tetrahedrite is stable from $4Cu_2S \cdot Sb_2S_3$ to Cu_3SbS_3 at 300°C and from $4Cu_2S \cdot Sb_2S_3$ to $Cu_{12}Sb_4S_{13}$ at 400°C. Whereas Skinner *et al.*[3] reported above 500°C a rapid shrinkage of the composition range for

97 tetrahedrite followed by its decomposition into $Cu_3Sb_1S_4$, Cu_3SbS_3 and Cu_xS (x going from
98 1.6 to 2) at 543°C, Il'yasheva[28] evidenced an incongruent melting for this phase at 574±2°C.
99 All the ternary phases are stable at 500°C.

100 The crystallographic data and the thermodynamic properties of the ternary solid
101 phases are given in Table 1 and Table 2, respectively.

102

Table I. Crystallographic data of the Cu-Sb-S ternary solid phases

Phase / Name	Crystal system	Space group	Lattice parameters (pm)	Reference
Cu_3SbS_4 /Famatinite	Tetragonal	I-42m	a=538.5,c=1075.4	[30]
$CuSbS_2$ /Chalcostibite	Orthorhombic	Pnma	a=601.8,b=379.58,c=1449.5	[32]
$Cu_{12}Sb_4S_{13}$ /Tetrahedrite	Cubic	I-43m	a=1032.4	[32]
Cu_3SbS_3 /Skinnerite	Monoclinic	$P2_1/c$	a=781.5,b=1025.2,c=1327.0	[33]

103

Table II. Thermodynamic properties of the Cu-Sb-S ternary solid phases from Ref. 34

Phase	Temperature	Δ_fG^0 (J/mol of atoms)	Δ_fH^0 (J/mol of atoms)	S^0 (J/K.mol of atoms)
Cu_3SbS_4	25°C	-207500 ± 3900	-200000 ± 6300	298 ± 18
$CuSbS_2$	25°C	-121400 ± 3400	-119000 ± 3500	148 ± 6.4
Cu_3SbS_3	25°C	-197800 ± 3800	-189300 ± 6500	269.5 ± 13.7

104

SUBSTITUTED TETRAHEDRITE: COMPUTATIONAL PART

Computational details

The calculations have been performed in the frame of the density-functional theory[35,36] using the gradient-corrected Perdew−Burke−Ernzerhof (PBE) exchange-correlation functionals.[37] All the structures have been relaxed to their equilibrium state and the energy and force thresholds have been fixed to 10^{-7} Ry and 10^{-4} Ry.bohr^{-1}, respectively. The projector augmented wave (PAW) method[38] has been used to treat nucleus and core and valence electrons interactions with cutoffs 48 Ry for the energy and 480 Ry for the density. A 4x4x4 k-point mesh has been utilized. The Quantum Espresso program package has been used for these calculations.[39]

The analysis of the bonding structure of the alloys has been performed using Bader's quantum theory of atoms in molecule[40] as implemented in the Critic2 program.[41]

Crystalline description of the tetrahedrite

The tetrahedrite crystal structure with stoichiometric formula $Cu_{12}Sb_4S_{13}$ is composed of two formula units and belongs to the body-centered cubic Bravais lattice with group number 217 (I-43m). It contains 29 atoms in the irreducible lattice located at five crystallographic sites. Copper atoms are in the two distinct Wyckoff positions (WP) 12e and 12d. Cu 12e is at the centre of a triangle formed by three sulphur atoms (two S in 24g WP and one S in 2a WP) and the assembly constitutes a trigonal plane. If one includes two antimony atoms on either sides of the plane the assembly is a trigonal bipyramid (Fig. 1a). It is noted that the Cu-Sb bond distance of this trigonal bipyramid is rather large with 3.536 Å and the Cu-S ones amount to 2.246 Å and 2.250 Å. It has been reported that, the weak bonding between Cu and Sb leads to soft vibrational modes of Cu having large anisotropic thermal motion, which could explain the low thermal conductivity of the tetrahedrite.[32,42] Six Cu

atoms in 12e WP are located nearby the centre of the lattice forming an octahedron around a sulphur atom in 2a Wyckoff position (Fig. 1b). The additional six Cu 12e atoms are located at the cube edges nearby the lattice corners occupied by S 2a atoms. Copper atoms in 12d WP form a tetrahedral arrangement with four sulphur atoms in 24g WP. They are located on the cube faces and form a square assembly with three other Cu atoms in 12d WP (Fig. 1c). The corresponding Cu-Cu distance is as large as 3.650 Å. The Cu-S distances are 2.311 Å and the S-Cu-S angles amount to 111.5°. As just mentioned the sulphur atoms in the 2a WP are located both at the corner and at the centre of the cubic lattice, and are at the centre of a regular octahedron formed with the Cu atoms in 12e WP (Fig. 1b). The Cu-S bond distances are 2.250 Å. Sulphur atoms occupying the 24g WP form a distorted tetrahedron with their neighbours, that are one Sb, two Cu 12d and one Cu 12e atoms, with bond distances of 2.452 Å, 2.311 Å and 2.246 Å, respectively (Fig. 1d). The antimony atoms are located in sites 8c and are surrounded by three sulphur 24g atoms, forming a pyramidal arrangement. As mentioned above the antimony atoms constitute the apex of a trigonal bipyramid for which Cu is the centre. It is noted that the height of the pyramid made of Sb and three S atoms is not aligned with that of the trigonal bipyramid but is tilted by 35.3°. The three Sb-S bond lengths equal 2.452 Å and the angles are 95.7°.

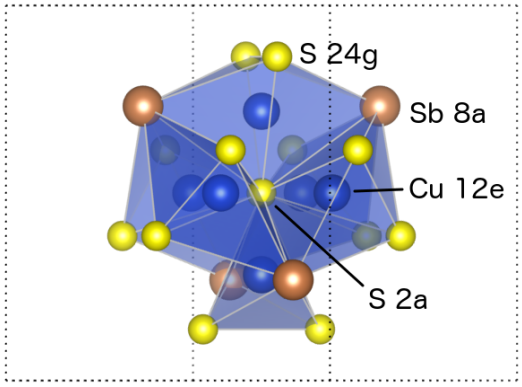

a) Copper *12e* at the centre of a trigonal bipyramid with S *2a*, S *24g* and Sb *8c* at the apex.

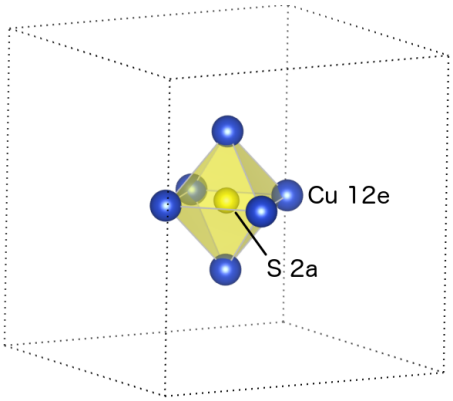

b) Sulphur *2a* at the centre of the lattice and at the center of an octahedron formed by six Cu *12e*.

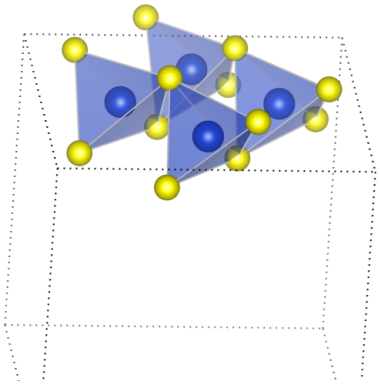

c) Copper *12d* arranged in square at the lattice face. They are located at the centre of a tetrahedron with S *24g* at the apex.

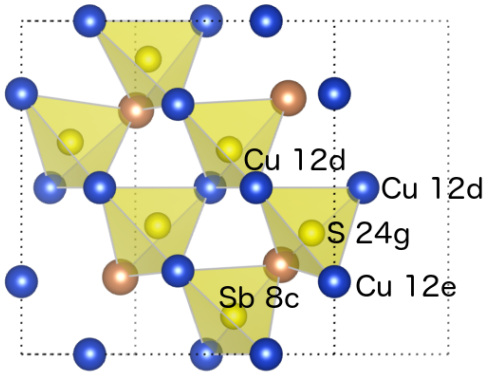

d) Sulphur *24g* in the centre of a distorted tetrahedron formed by two Cu *12d* (at the lattice face), one Cu *12e* (at the lattice edge) and one Sb *8c*.

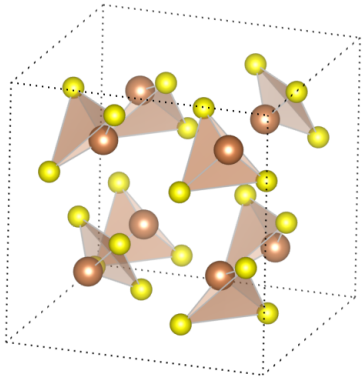

e) Antimony at the apex of a tetrahedron formed with three sulphur 24g atoms

Fig. 1: Structural features of the tetrahedrite. a) Environment of copper in *12e* Wyckoff position (WP); b) Environment of sulphur in *2a* WP; c) Environment of copper in *12d* WP; d) Environment of sulphur in *24g* WP; e) Environment of antimony in *8c* WP.

Procedure

The substituting elements considered in this work are Se and Te. The substituted atoms have been chosen as S and Sb ; S as a chalcogen and Sb since its replacement by Te has been evidenced in natural tetrahedrite.[43] As neither $Cu_{12}Sb_4Se_{13}$ nor $Cu_{12}Sb_4Te_{13}$ have been

reported in literature, in order to preclude a too big distorsion of the cell only the substitutions by one and two atoms per cell have been examined. The investigated compositions are the following ones : $Cu_{12}Sb_4S_{12.5}Se_{0.5}$, $Cu_{12}Sb_4S_{12}Se_1$,

$Cu_{12}Sb_{3.5}Se_{0.5}S_{13}$, $Cu_{12}Sb_3Se_1S_{13}$, $Cu_{12}Sb_4S_{12.5}Te_{0.5}$, $Cu_{12}Sb_4S_{12}Te_1$, $Cu_{12}Sb_{3.5}Te_{0.5}S_{13}$, $Cu_{12}Sb_3Te_1S_{13}$. The atom replacements on all the crystallographic sites (2a and 24g for S, 8c for Sb) have been envisaged. For 2 Te or Se atoms substitutions in the case of sulphur, three possible situations have been considered: 2 atoms at site S *24g*, one atom at site S *24g* and the other at site S *2a*, and 2 atoms at site S *2a*. For 2 Te or Se atoms substitutions in the case of antimony, since in pure tetrahedrite the eight antimony atoms form a somewhat distorted cube (hereafter called pseudo-cube) inside the cubic lattice, three possibilities have been considered: two atoms along the pseudo-cube edge, two atoms along the face diagonal of the pseudo-cube and 2 atoms along the principal diagonal of the pseudo-cube. The stability of the phases have been investigated by determining both the formation energies of the alloys using DFT calculations and the total and local volume changes using QTAIM ones.

The formation energies have been determined from the energies E calculated by DFT according to the following formula:

$$\Delta E_f = \frac{E(Cu_xSb_ySz_Xt) - xE(Cu) - yE(Sb) - zE(S) - tE(X)}{x+y+z+t} \quad (1)$$

Recalling that the number of formula in the unit cell of tetrahedrite is 2, a one-atom sulphur and antimony substituted tetrahedrite on the one hand and a two-atoms sulphur and antimony substituted tetrahedrite on the other hand correspond to $Cu_{12}Sb_4S_{12.5}X_{0.5}$, $Cu_{12}Sb_{3.5}X_{0.5}S_{13}$, and $Cu_{12}Sb_4S_{12}X$, $Cu_{12}Sb_3XS_{13}$, respectively.

Results

Formation energies and total lattice volume changes

Substitutions of Se and Te for S. The calculated values are given in Table 3. For a single substitution, both selenium and tellurium atoms prefer occupying site *24g*, the formation energies being –160.7 and –151.6 meV/atom respectively. The substitution at site *2a* is much less favourable by about 8 meV/atom. This preference for the *24g* site has already been experimentally evidenced for Se by Lu et al.[44] For two Te or Se atoms substitutions as mentioned above three possible situations have been envisaged: two atoms at site S *24g*, one atom at site S *24g* and the other at site S *2a*, and 2 atoms at site S *2a*. For the two former possibilities we observe that for a given substituting atom the energies are very close and actually lie in the error bar that we estimate to be 3-4 meV/atom. The 2-atoms substitution at site *2a* is the least preferential one for both Se and Te. We note that, the substitution with selenium is more preferred than that with tellurium, as the formation reactions pertaining to Se are more exothermic than those pertaining to Te.

These results show that whatever the substituting atom (Se or Te), the most favorable situation corresponds to a single atom substitution at site *24g* and that irrespective of the considered site, the replacement of S by Se is the most favorable one.

Table III: Formation energies (in meV/atom) and total volume change of the cell (in bohr^3) for 1 and 2 atoms Te or Se substitutions for sulphur. Columns 1 and 8 correspond to the ranking w.r.t. formation energies.

	Te substituted for S	ΔE_f	ΔV	ΔE_f	ΔV	Se substituted for S	
1	1 Te for S *24g*	–151.6	+1.297	–160.7	+0.093	1 Se for S *24g*	1
2	1 Te for S *2a*	–144.0	+2.452	–153.1	+0.312	1 Se for S *2a*	4
3	2 Te for 2 S *24g*	–136.7	+3.066	–155.5	+0.943	2 Se for 2 S *24g*	2
4	1 Te for S *24g* and 1 Te for S *2a*	–136.2	+3.976	–153.5	+0.685	1 Se for S *24g* and 1 Se for S *2a*	3
5	2 Te for 2 S *2a*	–127.3	+6.200	–144.7	+1.828	2 Se for 2 S *2a*	5

The total volume of the substituted structures changes sizeably with respect to that of pristine tetrahedrite as can be seen in Table 3. We observe that, except for 2-Se-atoms substitution, the more energetically favorable the site is, the smaller the volume change. In agreement with the respective atomic volumes of Se and Te atoms, sites substituted with Te are likely to be more affected, as we observe a larger total volume change, than when Se is the substituting element. It appears that, substitutions on site S *2a* induces more drastic changes in the total volume than those on site S *24g*, the volume change being about two to three times as large. As a consequence, the volume increase for 2-atoms substitution at site S *2a* is as large as +6 and nearly +2 Bohr^3 for Te and Se, respectively. These results on the volumes are in line with the energetic ones as they can lead to the same inferences as above.

Substitutions of Se and Te for Sb. The calculated values are given in Table 4. Remarkably enough, the formation energies are quite similar, suggesting therefore that both Se and Te may equally substitute for Sb. The most preferred substitution is by far obtained with one Se or Te atom only in place of antimony. The energy difference between the one-atom and two-atoms substitutions is above 20 meV/atom for both Se and Te, the largest energy difference being 23 meV/atom for Se. For two-atoms substitutions, the three configurations, namely two atoms along the pseudo-cube edge, two atoms along the face diagonal of the pseudo-cube and two atoms along the principal diagonal of the pseudo-cube, are energetically undistinguishable since the differences in formation energies lie in the error bar (3-4 meV/atom) ; they spread in the ranges [–122.2; –123.8] meV/atom and [–120.4; –122.5] meV/atom for Te and Se, respectively.

Regarding the total volume change of the lattice upon substitutions, it is remarkable that they are all negative irrespective of the substituting atom and configurations. The smallest volume change corresponds to the one-atom substitution. For two-atoms substitutions the situation is contrasted between Se and Te. For Se, the volume changes remain rather small (less than 2 $Bohr^3$). For Te, the two-atoms substitutions at the edge of the pseudo-cube still lead to the modest volume change of –2.6 $Bohr^3$. By contrast, a huge change is observed when two Sb atoms are replaced by Te on the pseudo-cube face and body diagonals. Notwithstanding this observation, the structures are not energetically destabilized as mentioned above.

Table IV: Formation energies (in meV/atom) and total volume change of the cell (in bohr^3) for 1 and 2 atoms Te or Se substitutions for antimony. Columns 1 and 8 correspond to the ranking w.r.t. formation energies.

	Te substituted for Sb	ΔE_f	ΔV	ΔE_f	ΔV	Se substituted for Sb	
1	1 Te for Sb *8c*	–144.8	–1.2	–143.4	–1.24	1 Se for Sb *8c*	1
2	2 Te for 2 Sb *8c* (pseudo-cube edge)	–123.8	–2.6	–122.5	–1.91	2 Se for 2 Sb *8c* (pseudo-cube edge)	2
3	2 Te for 2 Sb *8c* (pseudo-cube diagonal)	–123.6	–26.5	–120.7	–1.71	2 Se for 2 Sb *8c* (pseudo-cube diagonal)	3
4	2 Te for 2 Sb *8c* (pseudo-cube face diagonal)	–122.2	–36.1	–120.4	–1.93	2 Se for 2 Sb *8c* (pseudo-cube face diagonal)	4

Partial conclusions. From the formation energies viewpoint the most favourable situation corresponds to a single atom substitution, both Te and Se preferring replacing sulphur at the *24g* Wyckoff position to sulphur *2a* and antimony *8c* ones. Selenium is preferred for the sulphur substitution whereas tellurium and selenium are equally likely to replace antimony.

The lattice volume change is positive when substitutions occur at the sulphur sites, whereas it is negative at the antimony ones, the one atom substitution leading in all cases to the lower volume variation. For two-atoms substitutions, irrespective to the substituted element and site, Te leads to higher volume changes than Se. One can note that, whereas these volume variations are extremely large when Te substitutes for Sb, the energetic variations are quite small.

Local volume and atomic charge changes and electron density laplacian

In order to get better insight into the influence of substitutional atoms in the tetrahedrite, the atomic site volume and charge changes and electron density laplacian have been calculated using Bader's theory of atoms in molecules. Only one-atom substitutions are considered here since these lead to the structures bearing highest formation energies and smallest volume changes.

Pure tetrahedrite. The electron density laplacian of pure tetrahedrite in the (110) plane is depicted in figure 2. This plane contains S *2a* atoms (e.g. sulphur located at abscissa ca. 22), which are bonded to two copper *12e* (at abscissa ca. 20 and 24); the four remaining copper *12e* atoms that complete the octahedra around sulphur ones are located in two planes rotated by 45° from the (110) one and are thus not visible.

In the (110) plane, one can see that in agreement with the structure description already reported in literature, Cu *12e* is bonded to two S *24g* atoms and despite the long distance between copper *12e* and antimony atoms (3.536 Å, see above), these atoms are chemically bonded to each other since a bond path is found to connect them and a bond critical point (BCP) is found at the atomic basins boundary. Indeed, in the Bader's description the bonds are characterized by a path connecting two atoms, with b (see Fig. 2) depicting the position of the BCP where the electron density gradient vanishes.

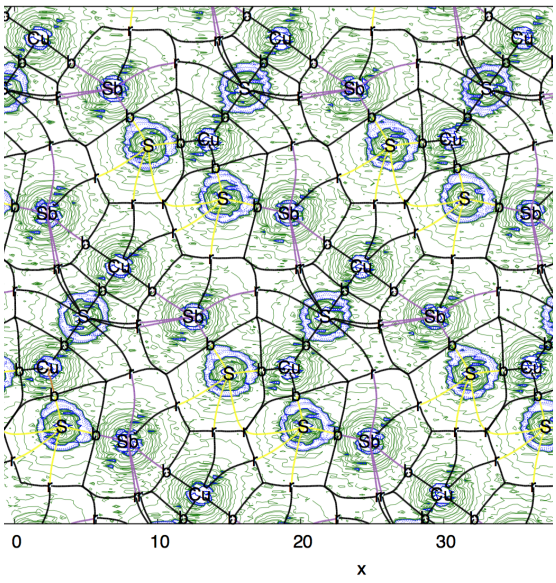

Fig. 2: Electron density laplacian of pure tetrahedrite. Legend. b: bond critical point; r: ring critical point; c: cage critical point. Color legend: electron accumulation in blue; electron depletion in green.

Substitutions of Se and Te for S *24g*. As one selenium atom replaces a sulphur *24g* atom, one of the Cu_{12e}-Sb bonds gets broken. This effect is observable as one compares Fig. 2 (at x=26) and Fig. 3a (at x=31). Important distortions in the structure are also observed, probably to accommodate the large size of Se: the Cu_{12e}-Se bond distance (2.541 Å) increases by 13% compared to the Cu_{12e}-S one; Cu *12e* moves out of the trigonal plane by about 20%; the angle Cu_{12e}-S_{2a}-Cu_{12e} of the octahedron height is 150° instead of 180°. One of the Cu_{12e}-Sb distances shortens by 20% (2.832 Å) while the other enlarges by 10% (3.896 Å) that leads to the bond breaking.

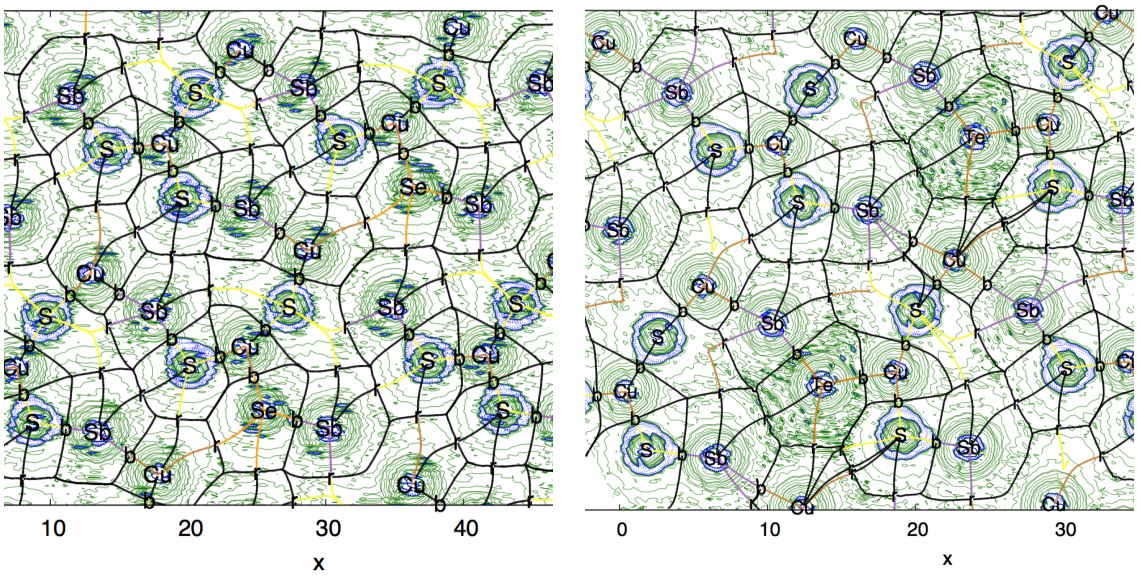

a) Se substitution for S *24g*

b) Te substitution for S *24g*

279 Fig. 3: Electron density laplacian of substituted tetrahedrite. a) Se substitution for S *24g*; b)
280 Te substitution for S *24g*. Legend. b: bond critical point; r: ring critical point; c: cage critical
281 point. Color legend: electron accumulation in blue; electron depletion in green.

282

Table V: Variation of the atomic charge (in electron charge unit) and atomic sites volume (in bohr^3) upon Se substitution for S *24g*.

	24g (S)	2a (S)	12e (Cu)	12d (Cu)	8c (Sb)
Δq	+0.01	+0.05	-0.01	-0.01	0
ΔV	+1.15	+5	-2.26	+0.45	-1.31

283

284 The effect of this replacement on the atomic charges and atomic volumes can be seen
285 in Table 5. Interestingly, sulphur *2a* is the most affected atom with a positive change of both
286 properties; a volume increase as large as +5 bohr^3 is observed. The Cu *12e* atom to which Se
287 is bonded is also affected, though in a lower extent and in the opposite way with a decrease of
288 both the volume and the charge. The site of the antimony atom to which Se is bonded

undergoes a volume decrease although its charge remains unchanged. The volume decrease is about the same in absolute value as the volume increase of the S *24g* site where the substitution occurs.

As Te substitutes for sulphur *24g* the same overall trends are observed as for Se. The graph of the electron density laplacian (Fig. 3b) shows that one of the Cu_{12e}-Sb is broken (3.592 Å, +1.2%) while the other one is strengthened (3.181 Å, –10%) and the octahedron around S *2a* is distorted (the Cu-S-Cu angle is 163°). However, we note that these structural changes are less drastic than for Se, although the Te substitution is energetically less favorable than the Se one. The volume change of the site *24g* of sulphur, where the Te substitution occurs, increases sizably (Table 6) by +3.3 $Bohr^3$ (2.9 times that for Se substitution) and the volume of the site *12d* (Cu) is almost twice as large as that for the Se substitution. Only the site *12e* of Cu undergoes a volume decrease of about the same amount as for Se substitution. These local volume changes explain why the overall volume of the structure increases (Table 3) as Te substitutes for sulphur.

We note finally that the atomic site charges vary in the same way and same extent as for the Se substitution.

Table VI: Variation of the atomic charge (in electron charge unit) and atomic sites volume (in $bohr^3$) upon Te substitution for S *24g*

	24g (S)	2a (S)	12e (Cu)	12d (Cu)	8c (Sb)
Δq	+0.01	+0.04	-0.01	-0.01	-0.01
ΔV	+3.3	+5.6	-2.1	+0.7	+0.2

Substitutions of Se and Te for Sb. The influence of the Se and Te substitutions for Sb on the electron density laplacian and bonding network of the tetrahedrite is depicted in figure 4a and 4b, respectively. Interestingly, as Se substitutes Sb a new chemical bond

appears between the selenium atom and the sulphur one of the *2a* site in spite of the large interatomic distance (4.027 Å); The bond is characterized by a bond path between both atoms and a bond critical point located *ca.* x=24 (Figure 4a). The Se-S_{2a} interatomic distance is 1.156 Å shorter than the Sb-S_{2a} one of the pure tetrahedrite. The appearance of this new bond implies a distortion of the octahedron around the S_{2a} atom; the Cu-S-Cu angle amounts to 153.07° and the sulphur atom moves out of the Cu_4 plane by 17.9° in the direction of Se. As to the case of the Te for Sb substitution, the bonding network of the structure is not affected compared to that of the pure tetrahedrite (Figure 4b). Some differences in the atomic charge and volume changes between these two types of substitutions can be observed (Tables 7 and 8). First, the atomic charges are barely varying upon Te substitution. By contrast, S_{2a} and Sb undergo significant increase and decrease, respectively, of their charge upon Se substitution, which can be correlated to the appearance of the new bond between these atoms.

The volumes are affected in various ways. For both Se and Te substitutions, the volume of S_{2a} increases drastically by up to 5 and 7 $Bohr^3$, respectively, and that of Cu_{12e} (bonded to S_{2a}) decreases by 2.5 $Bohr^3$, on average. The Cu_{12d} atoms being far from the substitution site, their volumes are not affected. As to the substituted site Sb, the volume decreases (increases) drastically (slightly) when Se (Te) is the substituting atom, these variations being in line with the differences in atomic sizes between Sb, Se and Te. Since the substitution at the Sb site is energetically equally plausible by Se and Te, we can infer that the total contributions to the formation energy of the various structural, electronic and bonding changes occuring in the structures are comparable.

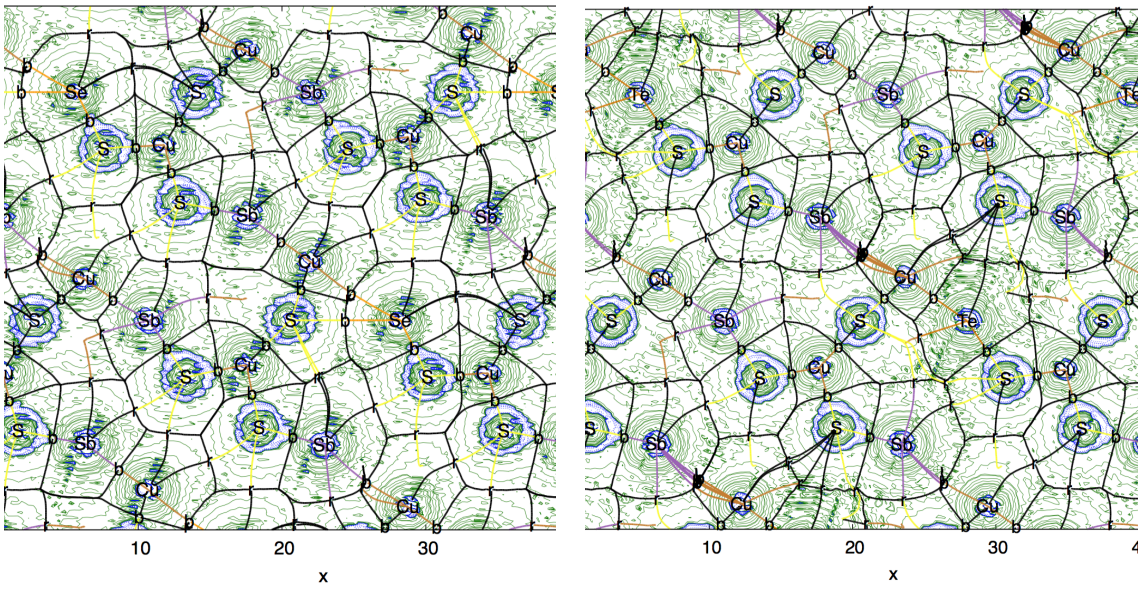

a) Se substitution for Sb *8c* b) Te substitution for Sb *8c*

Fig. 4: Electron density laplacian of substituted tetrahedrite. a) Se substitution for Sb *8c* ; b) Te substitution for Sb *8c*. Legend. b: bond critical point; r: ring critical point; c: cage critical point. Color legend: electron accumulation in blue; electron depletion in green.

Table VII: Variation of the atomic charge (in electron charge unit) and atomic sites volume (in bohr^3) upon Se substitution for Sb *8c*.

	24g (S)	2a (S)	12e (Cu)	12d (Cu)	8c (Sb)
Δq	+0.03	+0.05	-0.01	0	-0.06
ΔV	-0.90	+5.1	-2.32	0	-4.07

Table VIII: Variation of the atomic charge (in electron charge unit) and atomic sites volume (in bohr^3) upon Te substitution for Sb *8c*.

	24g (S)	2a (S)	12e (Cu)	12d (Cu)	8c (Sb)
Δq	+0.01	+0.01	0	+0.01	-0.02
ΔV	+0.60	+7.2	-2.7	-0.2	+0.6

Partial conclusions. Irrespective of both the substituting and the substituted atoms, the atomic charge changes are quite weak on all sites, the maximum being 0.06 electron charge unit. When substitution occurs on the S_{24g} site, irrespective of the substituting atom, charge change is only noticeable on the S_{2a} site. When substitution occurs on the Sb_{8c} site, the largest charge change occurs on this site while being weaker as Te substitutes for Sb.

Regarding the local volume changes, the S_{2a} site is the most impacted by both S_{24g} and Sb replacements. In all cases, the volume of the site S_{2a} increases. One can see that the volume of the site Cu_{12e}, which is adjacent to the site S_{2a}, decreases, though to a lesser extent. As one could expect, the impact of the substitution on the local volume changes is weaker when the site of interest is far from the substituted one (e.g. volume of the Cu_{12d} site when the replacement is on the Sb site).

The electron density laplacian shows few or even no chemical and structural modifications when Te substitutes for S_{24g} or Sb, respectively. In the case of Se, bigger structural distortions have been evidenced with the breaking of a Cu_{12e}-Sb bond when the substitution occurs on S_{24g} site and the formation of a Se-S_{2a} one when the substitution occurs on Sb site.

SUBSTITUTED TETRAHEDRITE: EXPERIMENTAL PART

DFT calculations of formation energies and total volume changes showed that : i) the most favourable situation corresponds to a single atom substitution, ii) selenium is preferred for the sulphur substitution whereas tellurium and selenium are equally likely to replace antimony, whereas QTAIM calculations evidenced larger structural and chemical distortions when Se is the substituting element irrespective of the substituted site. Since these results seem inconsistent, we experimentally investigated the following compositions: $Cu_{12}Sb_{3.5}Se_{0.5}S_{13}$, $Cu_{12}Sb_4S_{12.5}Te_{0.5}$ and $Cu_{12}Sb_{3.5}Se_{0.5}S_{12.5}Te_{0.5}$. We have not investigated $Cu_{12}Sb_{3.5}Te_{0.5}S_{13}$ and $Cu_{12}Sb_4S_{12.5}Se_{0.5}$ as these works were already done by Bouyrie et al.[45] and Lu et al.[44], respectively, and the authors found single-phased materials with a tetrahedrite structure.

Synthesis and characterization

The three aforementioned ternary and quaternary alloys have been prepared by mixing their constitutive elements with high purity grade in required proportion in evacuated (~10^{-2}Pa) sealed silica ampoules. The mixture was heated up to 680 °C and maintained at this temperature for 8 h. In order to get the equilibrium state, the samples have been quenched from melt in cold water and annealed at 400°C for about 150 h. The constitutive phases of the samples were evidenced by X-ray powder diffraction using a Bruker D8 Advance diffractometer with Cu-K□ radiation in the 2θ range from 5° to 80° and their proportion were evaluated by Rietveld refinement.

388 **Results**

389 The X-ray diffraction patterns for the three investigated samples are given in Figure 5
390 and the constitution of the alloys with the percentage of each phase determined by Rietveld
391 refinement are given in Table 9.

392 When one Te atom is substituted for a S one, the alloy is constituted of one phase only
393 which crystallizes in a tetrahedrite structure. As expected the lattice parameter of this phase (a
394 = 1036.1 pm) is larger than that of the pure sulphur tetrahedrite (a=1032.4 pm, see above).
395 When one Se atom is substituted for a Sb one, the alloy is constituted of two phases in an
396 equivalent ratio. One of these phases crystallizes in a tetrahedrite structure with a lattice
397 parameter a= 1034.3 pm, the other one crystallizes in a famatinite structure with the lattice
398 parameters a=539.0 pm and c=1076.1 pm which are larger than those of the pure sulphur
399 famatinite (a=538.5 pm and c=1075.4 pm, see above). When one Se atom is substituted for a
400 Sb one and one Te is substituted for a S one, the alloy is mainly constituted (95%) of a
401 tetrahedrite phase, the secondary phase (5%) crystallizing in a famatinite structure.

402 The whole results show that in spite of low formation energies and high volume
403 changes, alloys containing a tellurium atom at a sulphur site stabilize the tetrahedrite
404 structure. This statement is in agreement with the QTAIM calculations, which find lower
405 structural and chemical distortions when Te is the substituting element.

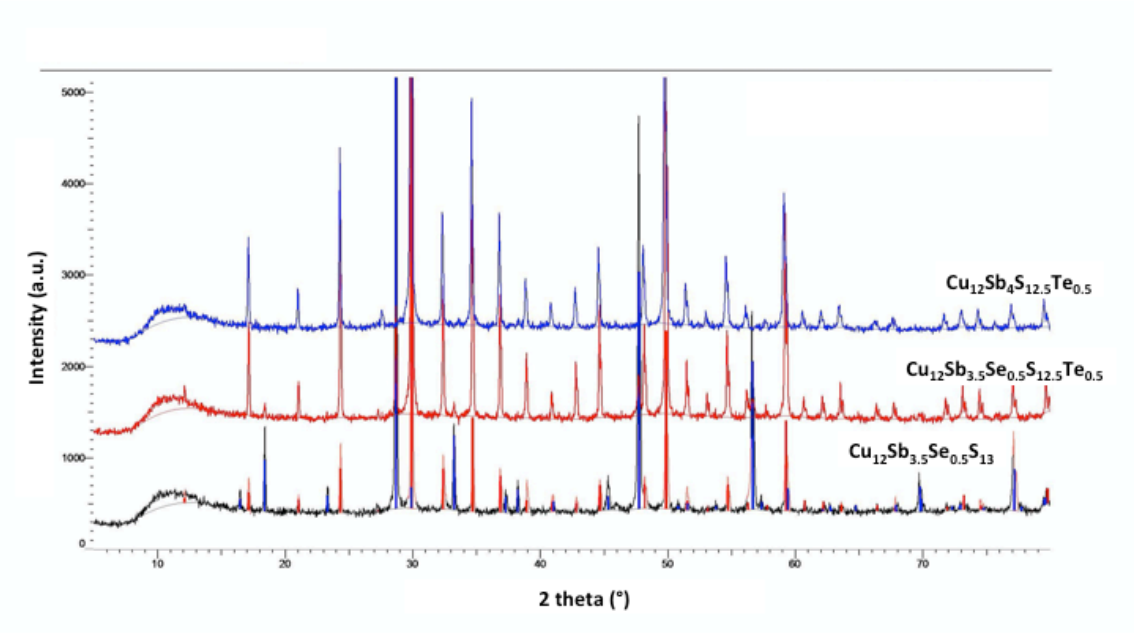

406

407 Fig. 5: X-ray diffraction patterns of $Cu_{12}Sb_4S_{12.5}Te_{0.5}$, $Cu_{12}Sb_{3.5}Se_{0.5}S_{13}$ and

408 $Cu_{12}Sb_{3.5}Se_{0.5}S_{12.5}Te_{0.5}$ alloys

409

Table IX: Constitution of the $Cu_{12}Sb_4S_{12.5}Te_{0.5}$, $Cu_{12}Sb_{3.5}Se_{0.5}S_{13}$ and $Cu_{12}Sb_{3.5}Se_{0.5}S_{12.5}Te_{0.5}$ samples and percentage of each phase determined by X-Ray diffraction measurements and Rietveld refinement.

Sample composition	Sample constitution (%)	
	Tetraedrite	Famatinite
$Cu_{12}Sb_4S_{12.5}Te_{0.5}$	100	0
$Cu_{12}Sb_{3.5}Se_{0.5}S_{13}$	45	55
$Cu_{12}Sb_{3.5}Se_{0.5}S_{12.5}Te_{0.5}$	95	5

410

411 **CONCLUSION**

412 In this work, we investigated Se and Te substitutions in tetrahedrite by coupling DFT

413 and QTAIM calculations. DFT calculations of formation energies and total volume changes

414 showed that the most favourable situation corresponds to a single atom substitution and that

selenium is preferred for the sulphur substitution whereas tellurium and selenium are equally likely to replace antimony. By contrast, QTAIM calculations evidenced irrespective of the substituted site, larger structural and chemical distortions when Se is the substituting element. In order to clarify these inconsistencies, we experimentally investigated three alloys and found that by contrast to a Se substitution for Sb, a Te susbtitution for S stabilizes the tetrahedrite structure. This investigation shows that a DFT calculation of formation energies and total volume changes is not sufficient to put forward conclusions on alloys stability. By giving chemical and structural information on a compound, in addition of being a good method to explain the structure-properties relationships, QTAIM appears as a valuable method to get information on phase stabilities.

ACKNOWLEDGEMENTS

This work is financially supported by China Scholarship Council (CSC N°201608530165). This work was granted access to the HPC resources of the Centre Informatique National de l'Enseignement Supérieur (CINES), Montpellier, France under allocation A0050806881 made by the Grand Equipement National de Calcul Intensif (GENCI). It was also granted access to the HPC resources of Aix-Marseille Université financed by the project Equip@Meso (ANR-10-EQPX-29-01) of the program "Investissements d'Avenir" supervised by the Agence Nationale de la Recherche.

REFERENCES

1. E. H. Roseboom, An investigation of the system Cu-S and some natural copper sulfides between 25 ° and 700 °C, *Econ. Geol.* 61, 641-672 (1966).
2. P.B. Barton, The Fe-Sb-S system, *Econ. Geol.* 66, 121-132 (1971).

439 3. B. J. Skinner, F. D. Luce, E. Makovicky, Studies of the sulfosalts of copper III.Phases
440 and phase relations in the system Cu-Sb-S, *Econ. Geol.* 67, 924-938 (1972).
441 4. P.B. Barton Jr., Solid solutions in system Cu-Fe-S. Part I: The Cu-S and CuFe-S joins,
442 *Econ. Geol.* 68, 455-465 (1973).
443 5. M. E. Fleet, Phase Equilibria at High Temperatures, *Rev. Mineral. Geochem.* 61, 365-
444 419 (2006).
445 6. F. Tesfaye Firdu, P. Taskinen, Thermodynamics and Phase Equilibria in the (Ni, Cu,
446 Zn)-(As, Sb, Bi)-S Systems at Elevated Temperatures (300–900°C), *Aalto University*
447 *Publications in Materials Science and Engineering* (2010).
448 7. S. Maske, B.J. Skinner, Studies of the sulfosalts of copper: I, Phases and phase
449 relations in the system Cu-As-S, *Econ. Geol.* 66, 901-918 (1971).
450 8]. R.W. Potter, An electrochemical investigation of the system copper-sulfur, *Econ.*
451 *Geol.* 72, 1524-142 (1977).
452 9. R.P. Elliot, Constitution of Binary Alloys 1st supplement, McGraw-Hill. New York
453 (1965).
454 10. M. Hansen, K. Anderko, Constitution of binary alloys. McGraw-Hill (1965).
455 11. T.B. Massalski, Cu–Sb (copper–antimony). In: Binary alloy phase diagrams, vol 2,
456 2nd edn. The Materials Information Society, Materials Park (1990).
457 12. V.F. Ross, The formation of intermediate sulfide phases in the solid state, *Econ. Geol.*
458 49, 734-752 (1954).
459 13. J.H. Wernick, K.E. Benson, New semiconducting ternary compounds, *J. Phys. Chem.*
460 *Solids* 3, 157-159 (1957).
461 14. L. Cambi, M. Elli, Processi Idrotermali-sintesi di solfosali da ossidi di metalli e
462 metalloidi 2 Cuprosolfoantimoniti, *Chimica &Industria* 47, 136-147 (1965).

15. R.A. Kuliev, A.N. Krestovnikov, V.M. Glazov, Phase Equilibrium and Intermolecular Interactions in Systems Formed by Copper and Antimony Chalcogenides, *Russ. J. Phys. Chem. (Engl. Transl.)* 43, 1721-1723 (1969).

16. R.A. Kuliev, A.N. Krestovnikov, V.M. Glazov, Phase equilibria between copper and antimony chalcogenides, *Izvest Akad Nauk Sssr Neorg Materialy* 5, 2217-2218 (1969).

17. A.A. Godovikov, Bismuth Sulfosalts : their chemical composition, synthesis and classification. In Pecularities of the chemical composition, synthesis, classification, *Nauka*, Moscow, Russia (1972).

18. N.A. Il'yasheva, Investigation of the system Cu_2S-Sb_2S_3 at 320-400°C, *Neorg. Mater.* 9, 1677-1679 (1973).

19. L.T. Bryndzia, A. M. Davis, Liquidus phase relations on the quasi-binary join Cu_2S-Sb_2S_3: Implications for the formation of tetrahedrite and skinnerite , *Amer. Mineral.* 74, 236-242 (1989).

20. M.I. Golovei, V.I. Tkachenko, M.Yu. Rigan, N.P. Stasyuk,Phase diagram of the system Cu_2S-Sb_2S_3 in the region of existence of $CuSbS_2$", *Neorg. Mater.* 26, 48-50 (1990).

21. S. Karup-Møller, E. Makovicky, Skinnerite Cu_3SbS_3, a new sulfosalt from the IIimaussaq alkaline intrusion, South Greenland, *Amer. Mineral* 59, 889-895 (1974).

22. H. J. Whitfield, Polymorphism in skinnerite Cu_3SbS_3, *Solid State Commun.* 33, 747-748 (1980).

23. A. Pfitzner, Disorder of Cu^+ in Cu_3SbS_3:structural investigations of the high- and low-temperature modification, *Z. Kristallogr.* 213, 228-236 (1998).

24. L. Pauling, E.W. Neuman, The crystal structure of binnite, $(Cu, Fe)_{12}As_4S_{13}$, and the chemical composition and structure of minerals of the tetrahedrite group, *Z. Kristallogr.* 88, 54-62 (1934).

25. K. Tatsuka, N. Morimoto, Tetrahedrite stability relations in the Cu-Sb-S system, *Econ. Geol.* 72, 258-270 (1977).

26. Y.A. Chang, J.P. Neumann, U.V. Choudary, Phase Diagrams and Thermodynamic Properties of Ternary Copper-Sulfur-Metal Systems, *Incra Monograph VII, The Metallurgy of Copper* (1979).

27. E. Makovicky, B.J. Skinner, Studies of the sulfosalts of copper VII. Crystal structures of the exsolution products $Cu_{12.3}Sb_4S_{13}$ and $Cu_{13.8}Sb_4S_{13}$ of unsubstituted synthetic tetrahedrite, *Can. Mineral.* 17, 619-634 (1979).

28. N.A. Il'yasheva, Peculiarities of tetrahedrite crystallization in the system Cu-Sb-S, *Neorg. Mater.* 20, 563-657 (1984).

29. T.-T. Chen, Compositional and thermal study on natural and synthetic phases in the system Ag_2S-Cu_2S-Sb_2S_3-Bi_2S_3, Degree of doctor, Cornell University (1971)

30. J. Garin, E. Parthé, The crystal structure of Cu_3PSe_4 and other ternary normal tetrahedral structure compounds with composition 13564, *Acta Cryst. B* 28, 3672-3674 (1972).

31. A. Kyono, M. Kimata, Crystal structures of chalcostibite ($CuSbS_2$) and emplectite ($CuBiS_2$): Structural relationship of stereochemical activity between chalcostibite and emplectite, *Am. Mineral.* 90, 162-165 (2005).

32. B. J. Wuensch, The crystal structure of tetrahedrite, $Cu_{12}Sb_4S_{13}$, *Z. Kristallogr.* 119, 437-453 (1964).

33. T. Balic Zunic, E. Makovicky, Determination of the crystal sructures of $TiPbSbS_3$, $(Ti,K)Fe_3(SO_4)_2(OH)_6$ and Cu_3SbS_3 from X-ray powder diffraction data, *Mat. Sci. Forum* 166-169, 659-664 (1994).

34. M. Babanly, Y. Yusibov, N. Babanly, The EMF Method with Solid State Electrolyte in the Thermodynamic Investigation of Ternary Copper and Silver Chalcogenides, Electromotive Force and Measurement in Several Systems, Publisher InTech (2011).

35. P. Hohenberg; W. Kohn, Inhomogeneous electron gas, *Phys. Rev.* 136, B864-B871 (1964).

36. W. Kohn, L.J. Sham, Self-Consistent Equations Including Exchange and Correlation Effects, *Phys. Rev.* 140, A1133-A1138 (1965).

37. J.P. Perdew, K. Burke, M. Ernzerhof, Generalized Gradient Approximation Made Simple, *Phys. Rev. Lett.* 77, 3865-3868 (1996).

38. P. E. Blöchl, *Phys. Rev. B* 50, 17953 (1994).

39. P. Giannozzi, S. Baroni, N. Bonini, et al., Quantum Espresso : a modular and open-source software project for quantum simulations of materials, *J. Phys.: Condens. Matter* 21, 395502 (2009).

40. R.F.W. Bader, Atoms in Molecules – A Quantum Theory, Oxford University Press, Oxford, (1990).

41. A. Otero-de-la-Roza, E. R. Johnson, V. Luaña, *Comput. Phys. Commun.* 185, 1007-1018 (2014).

42. W. Lai, Y. Wang, D.T. Morelli, X. Lu, *Adv. Funct. Mater.* 25, 3648-3657 (2015).

43. X. Lu, D.T. Morelli, Y. Xia, F. Zhou, V. Ozolins, H. Chi, X. Zhou, C. Uher, High Performance Thermoelectricity in Earth-Abundant Compounds Based on Natural Mineral Tetrahedrites, *Adv. Energy Mater.* 3, 342-348 (2013).

44. X. Lu, D. T. Morelli, Y.Wang, W. Lai, Y. Xia, V. Ozolins, Phase Stability, Crystal Structure, and Thermoelectric Properties of $Cu_{12}Sb_4S_{13-x}Se_x$ Solid Solutions, *Chem. Mater.* 28, 1781−1786 (2016).

45. Y. Bouyrie, C. Candolfi, V. Ohorodniichuk, B. Malaman, A. Dauscher, J. Tobola, B. Lenoir, Crystal structure, electronic band structure and high-temperature thermoelectric properties of Te-substituted tetrahedrites $Cu_{12}Sb_{4-x}Te_xS_{13}$ ($0.5 \leq x \leq 2.0$), *J. Mater. Chem. C* 3, 10476-10487 (2015).